frontiers | Frontiers in Physics

ORIGINAL RESEARCH
published: 05 May 2022
doi: 10.3389/fphy.2022.892215

Measurement of Anomalous Forces From a Cooper-Pair Current in High-T_c Superconductors With Nano-Newton Precision

M. Tajmar, O. Neunzig and M. Kößling*

Institute of Aerospace Engineering, Technische Universität Dresden, Dresden, Germany

Does a supercurrent drag space-time or generate a gravitational field that can be measured in a laboratory environment? A number of theories suggest that space-time itself could be modeled as a superfluid, so a current of Cooper-pairs might couple to its surroundings differently compared to non-quantum matter. On the other hand, experiments appeared in the literature suggesting that a discharge through a high-T_c superconductor generates a force beam, which can be picked up by external sensors. We developed a unique facility to investigate if such a link exists with unprecedented accuracy. Instead of measuring with sensors far away from the superconductor, we built a very precise thrust balance that features a cryostat allowing to measure any anomalous force directly from the superconducting source. An onboard battery and a wireless-controllable power supply as well as strict coaxial current leads ensure that any magnetic interaction with its surroundings is below the measurement noise. Our tests were done for both BSCCO and YBCO superconductors with and without the presence of a magnetic field parallel to the current flow. No force was seen within our resolution of around 100 nN for currents up to 15 A. This puts strong limits on all proposed theories and experimental claims.

Keywords: high-T_c superconductors, anomalous force, precision thrust balance, supercurrent-spacetime drag, nanonewton resolution

OPEN ACCESS

Edited by:
Giovanni Modanese, Free University of Bozen-Bolzano, Italy

Reviewed by:
C. S. Unnikrishnan, Tata Institute of Fundamental Research, India
George Hathaway, Hathaway Research International Inc, Canada

****Correspondence:***
M. Tajmar
martin.tajmar@tu-dresden.de

Specialty section:
This article was submitted to Condensed Matter Physics, a section of the journal Frontiers in Physics

Received: *08 March 2022*
Accepted: *13 April 2022*
Published: *05 May 2022*

Citation:
Tajmar M, Neunzig O and Kößling M (2022) Measurement of Anomalous Forces From a Cooper-Pair Current in High-T_c Superconductors With Nano-Newton Precision. Front. Phys. 10:892215. doi: 10.3389/fphy.2022.892215

INTRODUCTION

Does a supercurrent drag space-time or generate a gravitational field that can be measured in a laboratory environment? General relativity tells us that such experiments are impossible as we would need matter densities comparable to that of a neutron star moving close to the speed of light to produce effects that are comparable to Earth's gravitational acceleration [1]. Why should a quantum material like a superconductor make any difference? First of all, there is still no quantum theory of general relativity which may allow for deviations of classical predictions. And secondly, several theories have emerged, that propose that the fundamental physical vacuum [2–4] or space-time itself [5] can be viewed as a superfluid.

Have such anomalous interactions already been observed? Maybe the earliest hint was published by Tate et al [6, 7] on the attempt to measure the mass of a Cooper-pair in niobium, which disagreed with theoretical predictions by 92 ppm at an accuracy of 21 ppm. Recent measurements by Hoang et al [8] repeated those measurements for up to 6 superconductors, which reduced the gap to theoretical predictions, but given the increased accuracy with respect to Tate et al's experiments, this

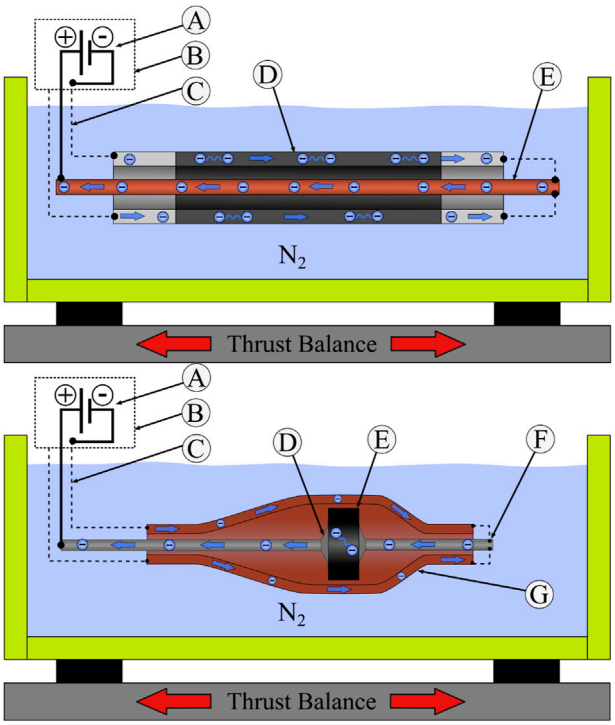

FIGURE 1 | Experimental setup inside a liquid/solid nitrogen reservoir with a coaxial electrical design to investigate thrust generation from cooper-pairs inside a High-T_c Superconductor. Top: **(A)** Current source; **(B)** Mumetal shield; **(C)** Coaxial cable; **(D)** BSCCO current lead; **(E)** Copper rod. Bottom: **(A)** Current source; **(B)** Mumetal shield; **(C)** Coaxial cable; **(D)** Indium solder joint; **(E)** YBCO bulk; **(F)** Inner wire AWG18; **(G)** Copper tube.

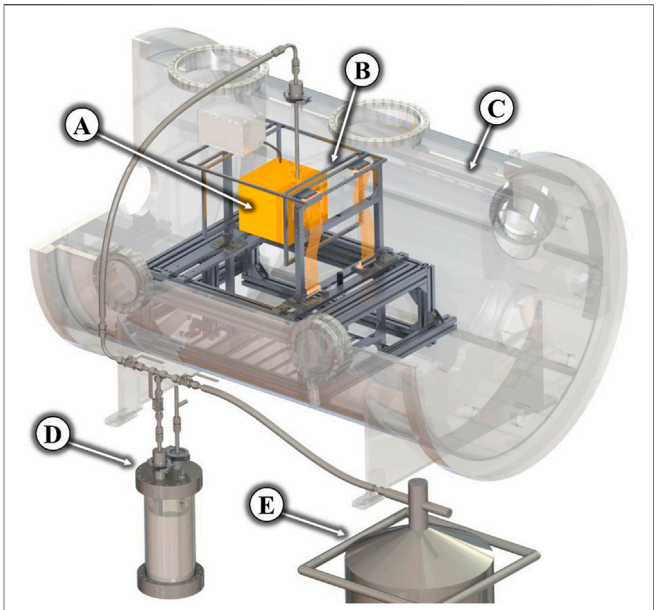

FIGURE 2 | Measurement setup with the cryo-box **(A)** on the thrust balance **(B)** inside the vacuum chamber **(C)** connected to a liquid nitrogen evaporator **(D)** and supplied by a dewar **(E)**.

disagreement is statistically even more significant. Again, for the case of niobium, the gap to predictions is now 18 ppm with an accuracy of only 2.1 ppm. Of course, a rather simple explanation is that those theoretical calculations need to be revised in order to match the new experimental data. However, another approach is to interpret this gap as evidence that non-classical quantum-gravity interactions may be possible. Tajmar and de Matos explored the possibility of anomalous space-time-dragging of rotating superconductors based on Tate's measurements [9, 10]. Subsequent weighting during the phase transition of bulk niobium and high-T_c superconductors did not show any anomaly [11], however, since the Cooper-pairs contribute very little to the bulk's mass, the Tate anomaly was not ruled out. Experiments to look for frame-dragging of spinning superconductors initially showed unexpected results that were picked up by fiberoptic gyroscopes [12], but refined measurements even with superfluid helium ruled out a gravity-like behavior and attributed the obtained results most likely to acoustic noise and vibration artefacts [13].

Nevertheless, there are two claims in the literature that suggest, that a current passing through a high-T_c superconductor does generate a force-beam that can be measured e.g. with an accelerometer. The first experiment was published by Podkletnov and Modanese [14], who described a setup, where a low pressure discharge from a capacitor array with up to 2000 kV and currents in the 10^4 A range on an YBCO disc was able to deflect a pendulum, that consisted of a cm-sized sphere 1 m away from the emitter, by up to 140 mm. Unfortunately, no visual evidence (photos, videos) was ever shown of the experiment making this extraordinary claim rather speculative. Hathaway [15] tried to replicate an earlier version of the Podkletnov experiment which did not reveal any anomalous force beam. The other claim was made by Poher [16–18], which is much better documented, who used a capacitor bank to directly discharge large currents through YBCO discs. He then observed a propulsive force with an accelerometer measuring several thousand Newtons for currents in the kA range. The force scaled with the discharge energy and therefore the current in the discharge. Both Podkletnov and Poher used specially-made two-layer YBCO discs with different critical temperatures. However, also normal YBCO discs are reported to work, although with a reduced effect.

Lörincz and Tajmar tested Poher's setup [19] and found out, that it is very difficult to shield the accelerometer and its electronics from the large electromagnetic impulse generated by an unshielded YBCO disc. Two separate double-Faraday cages, one for the capacitor bank and one for the accelerometer, as well as a completely isolated data acquisition setup was necessary to show, that the Poher effect was only an electromagnetic artefact.

Recently, we developed a very precise double-pendulum thrust balance with nano-Newton resolution that can support experiments up to 10 kg [20], which was even upgraded to allow for operating superconductors at cryogenic temperatures [21]. This gives us the possibility to investigate any superconductor/space-time drag/propulsive force link with

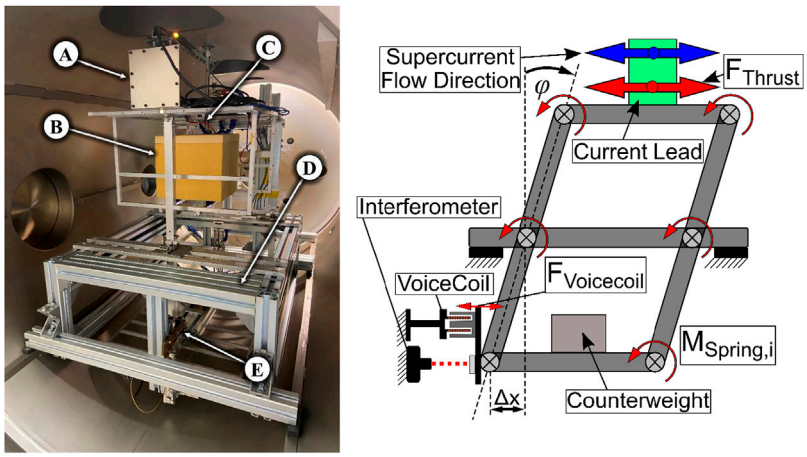

FIGURE 3 | Thrust Balance. Left: Electronics inside a mumetal housing **(A)** and the cryo-box **(B)** positioned below the liquid nitrogen outlet **(C)** on the thrust balance **(D)**, which is fixated with a bimetal actuator **(E)**. Right: Schematic illustration of the inverted counterbalanced double-pendulum principle. (adapted from **Figure 1A** in [20]).

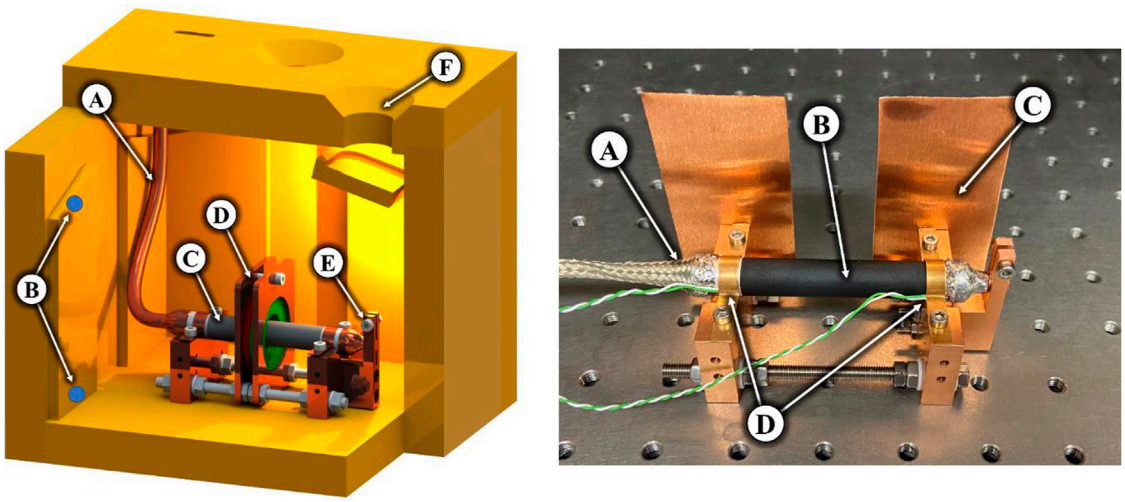

FIGURE 4 | BSCCO current lead. Left: CAD drawing of the superconducting current lead inside the cryo-box with a coaxial power feed clamped to a copper mount that increases thermal mass for prolonged measurement times and dissipates heat to the solid nitrogen. **(A)** Coaxial wire; **(B)** Liquid level indicators with two K-thermocouple; **(C)** BSCCO current lead; **(D)** Permanent magnet mount; **(E)** Copper mount; **(F)** Liquid nitrogen inlet. Right: Manufactured setup with the BSCCO current lead clamped to the copper mount and thermocouples attached to each end of the superconductor. **(A)** coaxial wire connection; **(B)** BSCCO current lead; **(C)** copper fins; **(D)** thermocouple positions.

unprecedented accuracy and in a much more systematic way. Instead of separating the anomalous force generation from the measurement device, we can now directly measure, if a high-T_c superconductor does generate a force during a discharge, which should be even higher, as it is directly measured from the source. With up to 15 A and an accuracy of a couple of tens of nano-Newtons, our ratio is approximately 5×10^{-9} N/A compared to the claim from Poher of approximately 1 N/A. In addition, we developed a novel coaxial design that eliminated almost all classical electromagnetic interactions providing reliable data. Our tests were done with standard YBCO and BSCCO superconductors manufactured by CAN superconductors.

EXPERIMENTAL SETUP

In order to measure if a supercurrent produces any anomalous propulsive effect while suppressing classical electromagnetic interactions, we chose to test our superconducting samples in a strictly coaxial configuration as illustrated in **Figure 1**. First, we tested a current lead made out of BSCCO (CSL-12/80.1 with 12 mm outer diameter, 80 mm length and 1 mm wall thickness, and silver coated contacts on both ends), where we inserted a copper rod in the middle and used a coaxial cable to connect the device to our power supply. In the YBCO configuration, a cylindrical bulk sample (CSYL-25 disc with 25 mm diameter

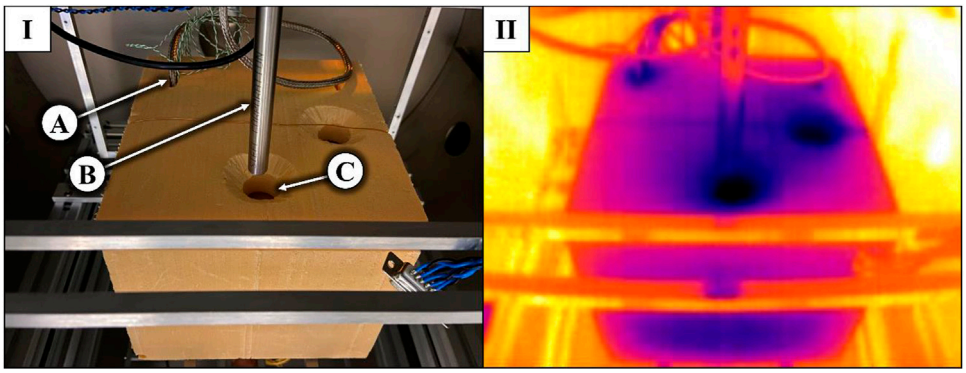

FIGURE 5 | Cryo-Box. Left: Field of view of the thermal camera focused to the XPS-Box and the surrounding structural components of the thrust balance. Right: Thermal camera image after the cooling process in vacuum to confirm thermal isolation from the balance. **(A)** inlet for coaxial wire and thermocouples; **(B)** liquid nitrogen feedthrough tube; **(C)** liquid nitrogen inlet.

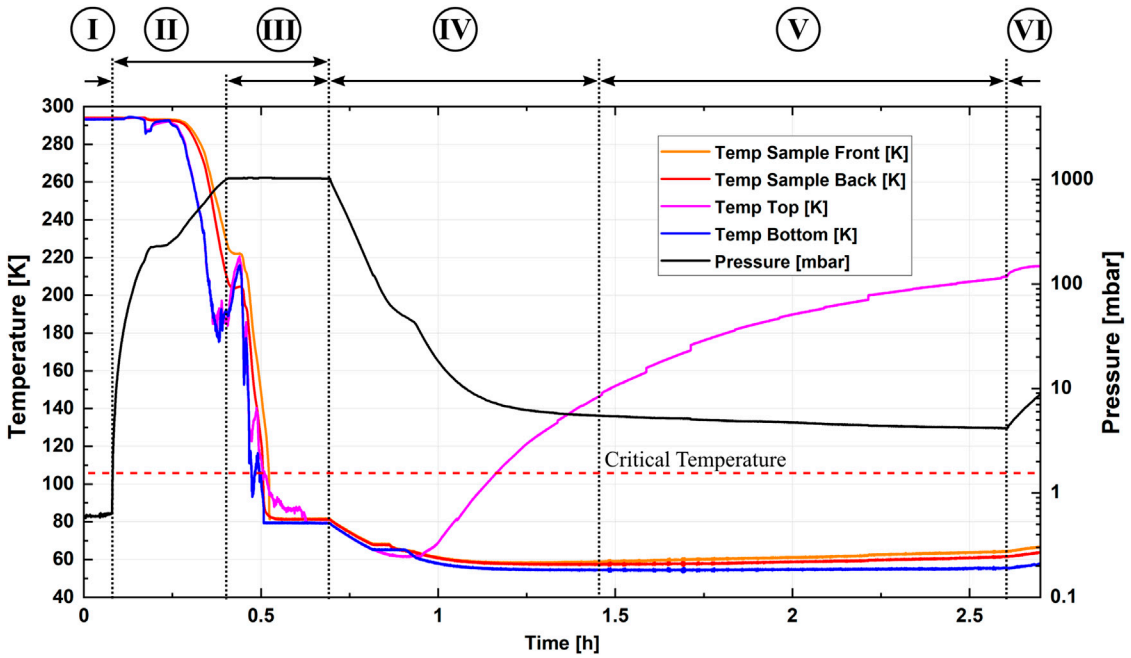

FIGURE 6 | Temperatures inside the cryo-box throughout the cooling process and thrust measurements. (I) Create vacuum. (II) Enable nitrogen evaporator to fill the chamber with nitrogen gas. (III) Cooling procedure of the setup and reservoir filling with liquid nitrogen at >125 mbar ambient pressure. (IV) Enable vacuum pump to further decrease N2 temperature and decrease convection for thrust measurements. (V) Thrust measurements at minimum temperature and chamber pressure with solid nitrogen. (VI) Measurement time-limit determined by the emptying nitrogen reservoir.

and 9 mm height) was placed in the middle of a copper tube. This ensures that the forward and backward flowing currents cancel each other, which eliminates magnetic fields very effectively. A gravitational/space-time dragging effect from the supercurrent would still be visible in an electromagnetic field-free environment.

The overall setup is illustrated in **Figures 2**, **3**. In order to test at low temperatures, the superconductor is mounted on the bottom of a cryo-box, which is made out of 2 cm thick extruded polystyrene (XPS) sheets featuring very low thermal conductivity. This box was fixed to the upper platform of a double-pendulum thrust balance in order to measure any propulsive effect. As shown in **Figure 2**, the thrust balance assembly was mounted inside a large vacuum chamber with a diameter of 0.9 m and a length of 1.5 m. In order to eliminate any ice formation due to water humidity, we had to pump down the chamber and fill it up with nitrogen gas before cooling. As this required a large amount of gas, we decided to use liquid nitrogen for this purpose too and added an evaporator with a small heater between dewar and vacuum chamber.

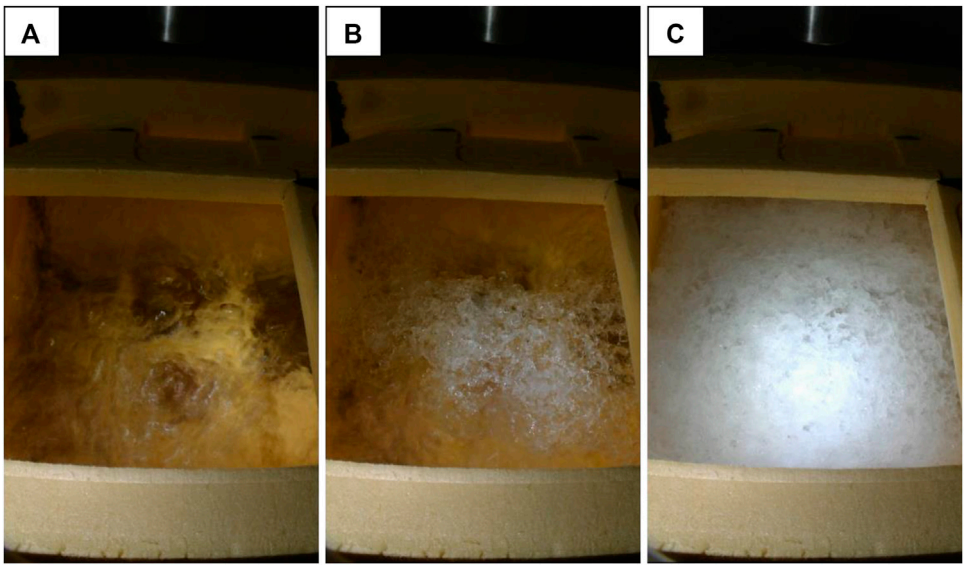

FIGURE 7 | Aggregate states of nitrogen inside the cryo-box. **(A)** Liquid nitrogen above 125 mbar; **(B)** Phase transition at triple point (125 mbar); **(C)** Solid nitrogen below 125 mbar.

TABLE 1 | Summary of All Measurements (BSCCO sample temperature did not change during testing).

Setup	Magnets	Sample Temperature [K] during On-Time	Electric current [A]	Measured Thrust
BSCCO Current Lead	No	57.35	10	(27 ± 63) nN
		58.35	11	(33 ± 97) nN
		58.05	12	(8 ± 52) nN
		57.65	13	(29 ± 85) nN
		57.85	14	(-6 ± 80) nN
		57.45	15	(5 ± 45) nN
	Yes	57.85	10	(7 ± 70) nN
		58.35	11	(28 ± 110) nN
		57.95	12	(–32 ± 96) nN
		57.75	13	(–25 ± 100) nN
		58.05	14	(43 ± 94) nN
		57.65	15	(–14 ± 92) nN
YBCO Bulk	No	68.58–72.78	5	(4 ± 62) nN
		77.45–86.65	10	(–3 ± 43) nN
	Yes	61.85–62.05	1	(–12 ± 81) nN
		63.15–67.6	5	(10 ± 25) nN
		69.02–79.15	10	(–27 ± 63) nN

The thrust balance uses a total of 9 friction-less torsion springs (C-Flex Bearing DD-10) in a counterbalanced inverted double-pendulum configuration, which leads to a defined displacement of a parallelogram, if a device under test produces a force as shown in **Figure 3**. This deflection is measured with an attocube IDS 3010 laser interferometer. It supports loads of up to 10 kg distributed on three structural beams, which rest on the torsional springs. The beams connect the upper and lower platforms where the experiment and counterweight are located respectively. Details on the balance and its calibration can be found in Refs. [20, 21]. Software-controlled damping, drift compensation and calibration through a voice-coil and precision current source complemented the overall balance system. A bimetal actuator was also added to fixate the balance during the cooling process.

In order to also eliminate any high-current-related measurement artefacts, a DPS 5015 power supply was directly mounted on the balance next to the cryo-box in a mu-metal shielded case. The power supply was controlled wirelessly using Bluetooth communication and powered by a battery pack. A LabJack T7 data acquisition system on the balance monitored the temperature of four K-type thermocouples, which were used to observe the sample temperature as well as to have an indicator for the liquid nitrogen level inside the cryo-box. An externally mounted FLIR thermal camera monitored the overall temperature environment of the experiment.

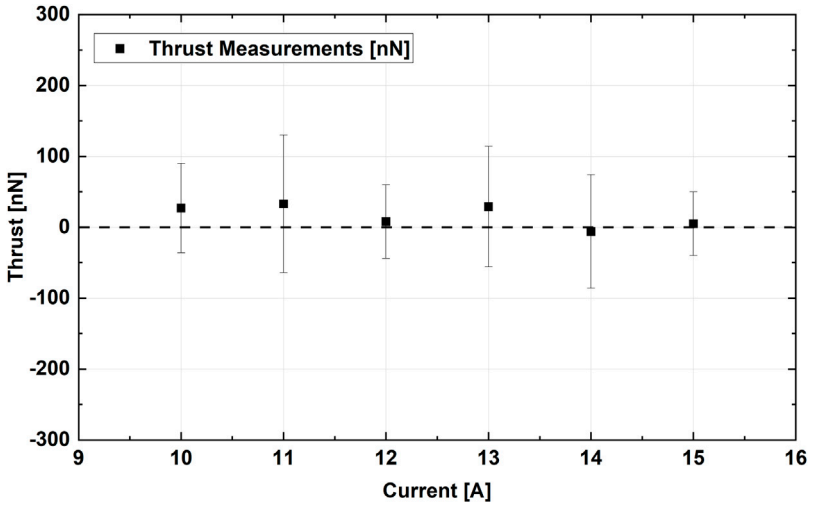

FIGURE 8 | Thrust measurements of the first BSCCO setup with increasing electric current levels between 10 and 15 A in steps of 1 A. Each data point represents an average of 2-3 consecutive measurements at equal operating parameters.

Liquid nitrogen entered the cryo-box through a hole with a little deflector below that redirected the flow towards the XPS walls and avoided direct spilling on the experiment to prevent damage from thermal shocks. **Figure 4** shows the BSCCO setup with copper fins mounted on a solid copper block, that ensured efficient heat dissipation even during nitrogen evaporation enabling sufficiently long test durations. The same copper mount and fins were used for the YBCO setup too. Finally, the box was mounted on sorbothane rubber pads to reduce vibration and to thermally isolate it from structural components of the balance, as shown in **Figure 5**.

The actual test procedure is illustrated in **Figure 6**:

1) We evacuated the chamber using an Edwards XDS35i scroll pump to approx. 0.6 mbar.
2) Then, we used the dewar and evaporator to fill up the chamber with dry nitrogen gas.
3) After reaching the phase transition pressure of 125 mbar during step 2, the cryo-box could be filled with liquid nitrogen. We were now waiting until the upper temperature indicator in the cryo-box reached 77 K after which we added still a few more milli-litre to account for nitrogen evaporation during the evacuation process in step 4.
4) As a liquid on the balance leads to strong vibrations which would severely limit our resolution, we now again activated

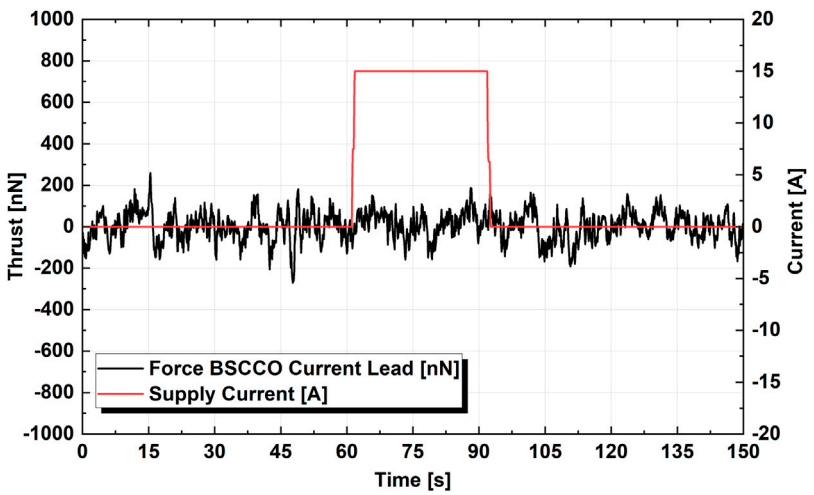

FIGURE 9 | Exemplary thrust measurement of the BSCCO current lead at a maximum current of 15 A.

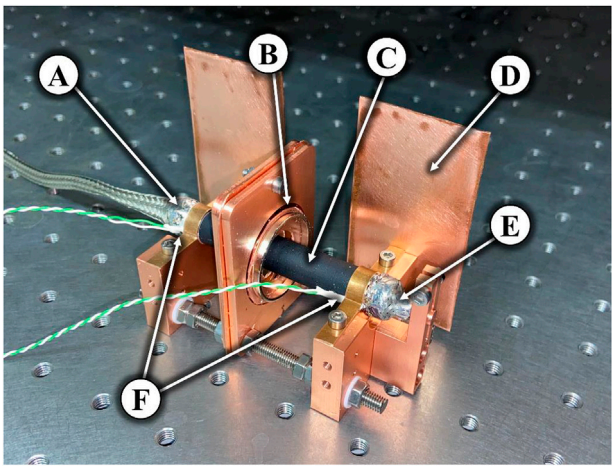

FIGURE 10 | Enhanced setup with three axially magnetised neodymium 30UH permanent magnet rings positioned coaxially to the current lead. **(A)** Coaxial wire connection; **(B)** Permanent magnet ring; **(C)** BSCCO Current Lead; **(D)** Copper fins; **(E)** Coaxial wire; **(F)** Thermocouple positions.

the vacuum pump and lowered the pressure to around 4 mbar (limited by our pumping speed) which turned the liquid nitrogen into solid ice by performing another phase transition below 125 mbar. In addition, the temperature was lowered to around 60 K, which was well below the critical temperatures of both BSCCO (108 K) and YBCO (92 K).

5) Now the setup was ready for thrust measurements, which could last up to 1 hour before too much nitrogen evaporated requiring a repetition of the cooling process.

By removing the top cover of the cryo-box and using a camera, we were able to observe the different states of nitrogen in the box turning from a boiling liquid to a solid as shown in **Figure 7**. Solid nitrogen was similar to snow with small voids in between, which limited effective cooling.

TEST RESULTS

We decided to test both BSCCO and YBCO superconductors with and without the addition of a strong permanent magnetic field in the direction of the current flow as Podkletnov did use a similar configuration but Poher did not. Moreover, some recent theoretical work by Inan suggests that a magnetic field may be necessary for superconductors as a pre-condition for gravitational experiments [22]. Our maximum current always stayed below the critical current listed for both superconductors also in the presence of the magnetic field. A summary of all test results is shown in **Table 1** for both high-T_c superconductors respectively.

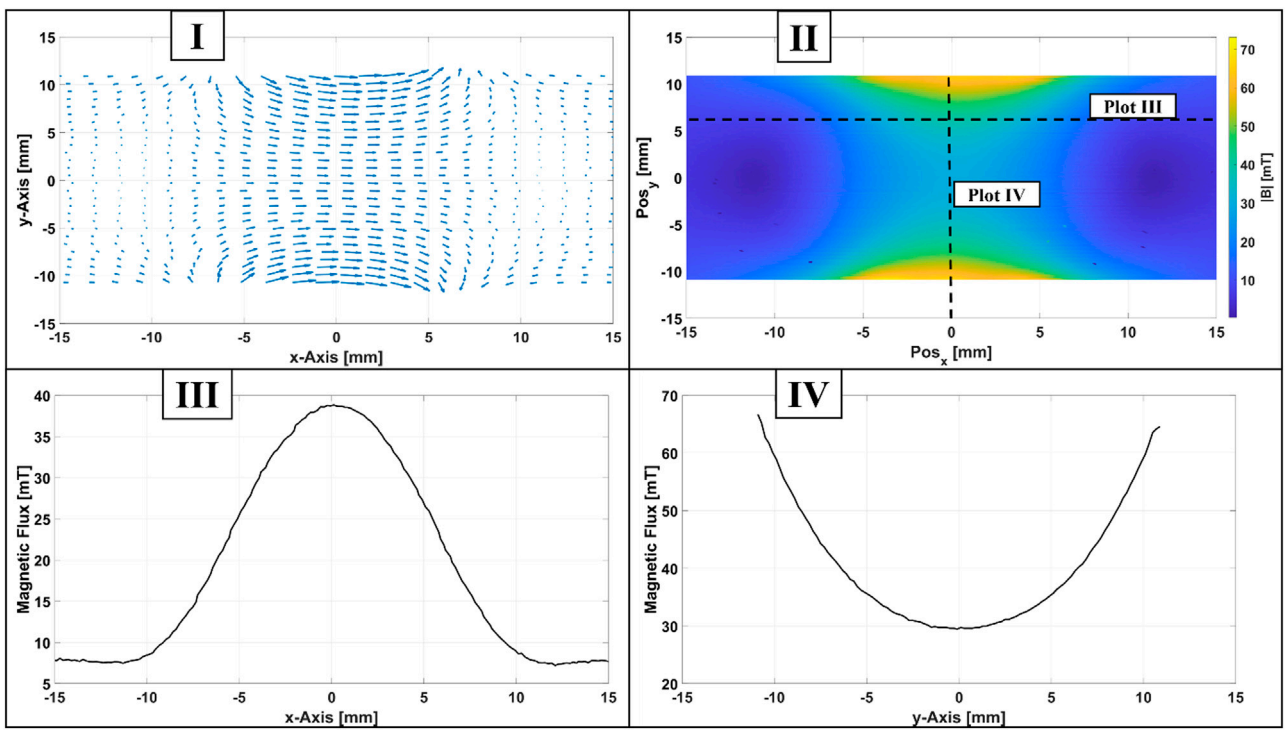

FIGURE 11 | Magnetic field measurement results from the BSCCO setup: **(I)** Vector diagram of the magnetic flux in 2D; **(II)** Magnetic flux intensity in 2D along the centre plane; **(III)** Magnetic flux values plotted vertically along the central region in the magnet array; **(IV)** Magnetic flux values plotted horizontally at 6 mm distance to the ring centre where the current lead is located during thrust measurements.

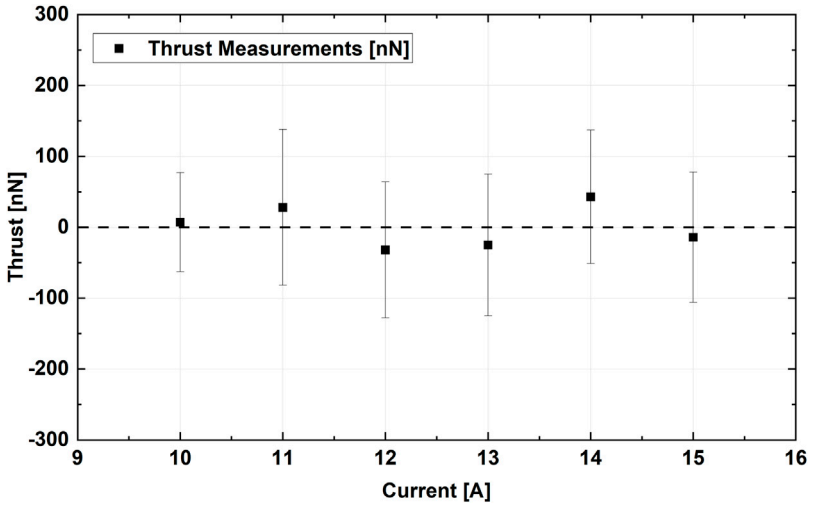

FIGURE 12 | Thrust measurements of the enhanced BSCCO setup with magnet rings with increasing electric current levels between 10 and 15 A in steps of 1 A. Each data point represents an average of 2-3 consecutive measurements at equal operating parameters.

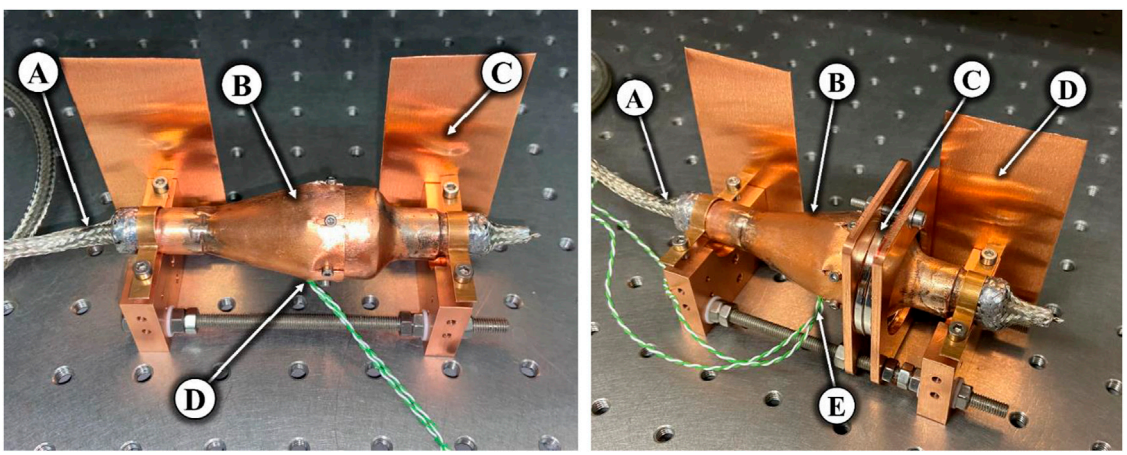

FIGURE 13 | YBCO Bulk Setup. Left: Manufactured setup with the YBCO bulk inside a tapered copper housing clamped to the copper mount and thermocouples attached to the superconductor. **(A)** Coaxial wire connection; **(B)** Copper housing; **(C)** Copper fins; **(D)** Thermocouple outlet. Right: Enhanced YBCO setup with two axially magnetised neodymium 30UH permanent magnet rings positioned coaxially to the superconductor. **(A)** Coaxial wire connection; **(B)** Copper housing; **(C)** Permanent magnet rings; **(D)** Copper fins; **(E)** Thermocouple outlet.

The silver coatings at both ends from the BSCCO current lead enabled a good electric contact such that we could use the maximum current from our power supply of up to 15 A. **Figure 8** shows the thrust measurements between currents ranging from 10 to 15 A indicating a null effect within our measurement resolution of a couple of tens of nano-Newtons. Each data point is an average of 2-3 single measurements in order to increase statistical significance. A single thrust measurement at 15 A can be seen in **Figure 9**. The overall profile length was set to 150 s with an operating time of 30 s starting at 60 s. No change of the thrust signal can be seen either during transients (on/off) or along the profile.

Figure 10 illustrates the addition of permanent magnet rings in the middle of the BSCOO tube. We used three NdFeB rings with grade 30 UH (outer diameter 30.5 mm, inner diameter 27.5 mm and length 3 mm), which were characterized using a hall-effect sensor (TLE493D-W286) mounted on a CNC table for automated data acquisition. The whole magnetic field strength around the ring area can be seen in **Figure 11**, indicating a maximum field strength of approximately 40 mT at the position of the BSCCO outer diameter. The addition of the magnetic field had no effect on the measurement as shown in **Figure 12**.

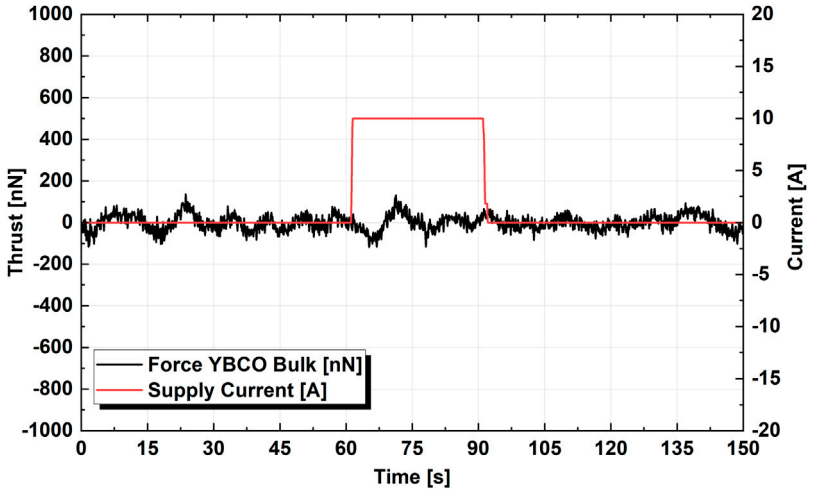

FIGURE 14 | Thrust measurement of the YBCO bulk at a maximum current of 10 A.

All measurements were repeated for our YBCO configuration. Here, we used indium, which was heated and soldered to the surface to establish the electric contact at both ends. As excessive heat from soldering electrical contacts could lead to permanent damage of the YBCO bulk, we verified the superconducting properties by field cooling a permanent magnet to the YBCO disc after the soldering process. However, this contacting method only allowed a maximum current of 10 A. Due to the larger diameter of the YBCO sample, we had to use larger magnetic rings too (two rings with outer diameter 45 mm, inner diameter 39 mm, 3 mm, grade 30 UH) resulting in a maximum field strength at the YBCO outer surface of 52 mT. **Figures 13**, **14** summarize the setup all measurements indicating again a null effect in both non-magnet and magnet setups.

CONCLUSION

We developed a novel and high-accuracy experimental setup that allows testing, if a supercurrent through a high-T_c superconductor produces any anomalous propulsive effect. Great care was taken on eliminating electromagnetic interactions using a strict coaxial configuration that were believed to be responsible for previous claims [19]. Our accuracy was at or below 100 nN, which is around 9 orders of magnitude below some of the claims in the literature [16–18] if normalized by the currents used. Our work used currents up to 15 A and standard off-the-shelve BSCCO and YBCO superconductors. Although this may not completely resemble the conditions used by others, the high resolutions further strengthens our previous assessment that electromagnetic artefacts have been a dominating error source in past experiments.

Our results may be used to test against a variety of emerging theoretical concepts that link quantum materials to gravity and space-time interactions.

DATA AVAILABILITY STATEMENT

The original contributions presented in the study are included in the article/Supplementary Material, further inquiries can be directed to the corresponding author.

AUTHOR CONTRIBUTIONS

MT had the idea for the experiment and wrote the paper, ON designed the balance and carried out the thrust measurements, ON and MK designed the superconductor experiments and MK performed the magnetic field measurements.

REFERENCES

1. Forward R. General Relativity for the Experimentalist. *Proc. IRE* (1961) 49(5): 892–904. doi:10.1109/jrproc.1961.287932
2. Sinha KP, Sudarshan ECG. The Superfluid as a Source of All Interactions. *Found. Phys.* (1978) 8(11–12):823–31. doi:10.1007/bf00715056
3. Volovik GE. The Superfluid Universe. In: *Novel Superfluids*, K-H Bennemann JB Ketterson, editors. Oxford University Press (2013). p. 570–618. doi:10.1093/acprof:oso/9780199585915.003.0011
4. Huang K. *A Superfluid Universe*. World Scientific (2016).
5. Liberati S, Maccione L. Astrophysical Constraints on Planck Scale Dissipative Phenomena. *Phys. Rev. Lett.* (2014) 112(15):151301–5. doi:10.1103/PhysRevLett.112.151301
6. Tate J, Cabrera B, Felch SB, Anderson JT, "Precise Determination of the Cooper-Pair Mass," *Phys. Rev. Lett.*, 62, no. 8, pp. 845–8. 1989.doi:10.1103/physrevlett.62.845
7. Tate J, Felch SB, Cabrera B, 1990, "Determination of the Cooper-pair Mass in Niobium," *Phys Rev B Condens Matter*, 42, no. 13, pp. 7885–93. 1990.doi:10.1103/physrevb.42.7885

8. Hoang LP, Le D-N, Pham DA, Nguyen TKC, Nguyen TMA, Ngo XC, et al. High-precision Measurement of Cooper-pair Mass Using Rotating Spherical-Shell Superconductor. *Mater Lett* (2020) 262:127176. doi:10.1016/j.matlet.2019.127176
9. Tajmar M, De Matos CJ. Gravitomagnetic Field of a Rotating Superconductor and of a Rotating Superfluid. *Phys C Supercond* (2003) 385(4):551–4. doi:10.1016/s0921-4534(02)02305-5
10. Tajmar M, De Matos CJ. Extended Analysis of Gravitomagnetic Fields in Rotating Superconductors and Superfluids. *Phys. C Supercond. its Appl.* (2005) 420(1–2):56–60. doi:10.1016/j.physc.2005.01.008
11. Tajmar M, Plesescu F, Seifert B. Measuring the Dependence of Weight on Temperature in the Low-Temperature Regime Using a Magnetic Suspension Balance. *Meas. Sci. Technol.* (2010) 21(1):015111. doi:10.1088/0957-0233/21/1/015111
12. Tajmar M, Plesescu F, Seifert B. Anomalous Fiber Optic Gyroscope Signals Observed above Spinning Rings at Low Temperature. *J. Phys Conf. Ser.* (2009) 150(3):032101. doi:10.1088/1742-6596/150/3/032101
13. Tajmar M. Evaluation of Enhanced Frame-Dragging in the Vicinity of a Rotating Niobium Superconductor, Liquid Helium and a Helium Superfluid. *Supercond. Sci. Technol.* (2011) 24(12):125011. doi:10.1088/0953-2048/24/12/125011
14. Podkletnov E, Modanese G. Investigation of High Voltage Discharges in Low Pressure Gases through Large Ceramic Superconducting Electrodes. *J. Low Temp. Phys.* (2003) 132(3–4):239–59. doi:10.1023/a:1024413718251
15. Hathaway G. Experimenting with Novel Propulsive Ideas. In: *Estes Park Advanced Propulsion Workshop*. H Fearn LL Williams, editors. Mojave: The Space Studies Institute (2016). p. 21–44.
16. Poher C, Poher D, Marquet P. Withdrawn Article - Propelling Phenomenon Revealed by Electric Discharges into Layered Y123 Superconducting Ceramics. *Eur. Phys. J. Appl. Phys.* (2010) 50(3):30803. doi:10.1051/epjap/2010060
17. Poher C, Poher D. Physical Phenomena Observed during Strong Electric Discharges into Layered Y123 Superconducting Devices at 77 K. *Appl. Phys. Res.* (2011) 3(2):51–66. doi:10.5539/apr.v3n2p51
18. Poher C, Modanese G. Enhanced Induction into Distant Coils by YBCO and Silicon-Graphite Electrodes under Large Current Pulses. *Phys. Essays* (2017) 30(4):435–41. doi:10.4006/0836-1398-30.4.435
19. Lörincz I, Tajmar M, "Null-Results of a Superconducting Gravity-Impulse-Generator," Proceedings of the 52nd AIAA/SAE/ASEE Jt. Propuls. Conf., p. AIAA. (2016). 2016–4988. Salt Lake City, UT July 2016.doi:10.2514/6.2016-4988
20. Tajmar M, Neunzig O, Weikert M. High-accuracy Thrust Measurements of the EMDrive and Elimination of False-Positive Effects. *CEAS Space J* (2022) 14(1):31–44. doi:10.1007/s12567-021-00385-1
21. Neunzig O, Weikert M, Tajmar M. Thrust Measurements of Microwave-, Superconducting- and Laser-type Emdrives. *Acta Astronaut* (2022). 14:583–595. doi:10.1016/j.actaastro.2022.02.014
22. Inan N, *Superconductor Meissner Effects for Gravito-Electromagnetic Fields in Harmonic Coordinates Due to Non-relativistic Gravitational Sources*. Available at: https://www.frontiersin.org/articles/10.3389/fphy.2022.823592/abstract (Accessed November 4, 2022). 2022.

Conflict of Interest: The authors declare that the research was conducted in the absence of any commercial or financial relationships that could be construed as a potential conflict of interest.

Publisher's Note: All claims expressed in this article are solely those of the authors and do not necessarily represent those of their affiliated organizations, or those of the publisher, the editors and the reviewers. Any product that may be evaluated in this article, or claim that may be made by its manufacturer, is not guaranteed or endorsed by the publisher.